Polarized QED cascades

Daniel Seipt, 1,2,3,* Christopher P. Ridgers, Dario Del Sorbo, and Alec G. R. Thomas Helmholtz Institut Jena, Fröbelstieg 3, 07743 Jena, Germany

2 GSI Helmholtzzentrum für Schwerionenforschung GmbH,

Planckstrasse 1, 64291 Darmstadt, Germany

3 The Gérard Mourou Center for Ultrafast Optical Science,

University of Michigan, Ann Arbor, Michigan 48109, USA

4 York Plasma Institute, Department of Physics,

University of York, York YO10 5DD, United Kingdom

5 High Energy Density Science Division,

SLAC National Accelerator Laboratory, Menlo Park, CA 94025, USA

(Dated: April 26, 2022)

Abstract

By taking the spin and polarization of the electrons, positrons and photons into account in the strong-field QED processes of nonlinear Compton emission and pair production, we find that the growth rate of QED cascades in ultra-intense laser fields can be substantially reduced. While this means that fewer particles are produced, we also found them to be highly polarized. We further find that the high-energy tail of the particle spectra is polarized opposite to that expected from Sokolov-Ternov theory, which results from "spin-straggling". We employ a kinetic equation approach for the electron, positron and photon distributions, each of them spin/polarization-resolved, with the QED effects of photon emission and pair production modelled by a spin/polarization dependent Boltzmann-type collision operator. For photon-seeded cascades, depending on the photon polarization, we find an excess or a shortage of particle production in the early stages of cascade development, which provides a controllable experimental signature.

^{*} d.seipt@hi-jena.gsi.de

I. INTRODUCTION

The ongoing development of high-power petawatt class lasers [1] has already opened new avenues for high-intensity laser-plasma physics. Already with present day laser technology the effect of QED process can be observed in high-intensity laser-matter interactions [2–4]. With the upcoming generation of multi-10 PW laser systems [5, 6] it is expected that laser-plasma interactions will enter a novel regime of QED plasma physics where strong-field QED process such as high-energy photon emission via nonlinear Compton scattering and electron-positron photo-production will play an important role for the overall dynamics of the plasmas [7].

One of the most striking predictions of strong-field QED [8, 9] is the formation of avalanche-type QED cascades [10] at laser intensities approaching 10^{24} W/cm². In these cascades the prolific generation of high-energy photons and electron-positron pairs can convert an initially strong laser field into a hot and dense plasma of electrons, positrons and photons. One of the conclusions drawn from these predictions was that the Schwinger field $E_S = 1.3 \times 10^{18}$ V/m [11] is then difficult to reach because of laser field depletion during the cascade [12–14].

In a cascade, efficient pair production is facilitated by hard photons which have a quantum parameter $\chi_{\gamma} \gtrsim 1$. A particle with four-momentum p^{μ} has quantum parameter $\chi = e|F^{\mu\nu}p_{\nu}|/m^3$, where $F^{\mu\nu}$ is the EM field strength tensor, e the elementary charge and m the electron mass. Those photons, in turn, are emitted by leptons, i.e. electrons and positrons, with $\chi_e \gtrsim 1$, leading to exponential increases in particle number [10, 12, 15–20]. A renewable supply of sufficiently many leptons with $\chi_e \gtrsim 1$ necessarily can be provided if the electric field of the laser is capable of accelerating low-energy leptons with $\chi_e \ll 1$ to $\chi_e \gtrsim 1$.

This is one of the decisive features in avalanche-type cascades, which can occur, for instance, in rotating electric fields at the magnetic nodes for two counter-propagating circularly polarized laser pulses [10]. Such an avalanche-type cascade exhibits an exponential growth in particle number, limited by the available (laser) field energy. By contrast, in shower-type cascades that occur in interactions of of high-energy particle with non-accelerating field configurations, such as in collisions with (nearly) plane-wave laser pulses, the leptons are not reaccelerated to $\chi_e \gtrsim 1$, and therefore the cascade multiplicity is limited by the maximum

initial particle energy [21–23].

QED pair-cascades are important in extreme astrophysical environments, where they may develop in matter, photon gas and magnetic field backgrounds [24]. In the latter case of cascades in strong magnetic fields, as found in pulsar atmospheres [25, 26], the same basic theoretical framework to describe the quantum processes is used for describing laser-plasma interactions [27]. There has been significant recent progress in understanding important physics details of cascades, including aspects of laser polarization, field structure [28–30] and seeding [31, 32].

Lepton spin- and polarization effects in strong-field QED(-plasma) processes have gained some significant recent interest [33–40], (even though some fundamental scattering cross sections in strong laser fields were calculated much earlier [41, 42]). It was shown that electron beams colliding with bi-chromatic laser pulses can self-polarize due to hard-photon emission [36], and that positrons generated by these photons are polarized as well [38]. Alternatively, it was proposed to collide electron beams with elliptically polarized laser pulses to generate polarized lepton jets [37, 39]. The radiative self-polarization of electrons in rotating electric fields in analogy to the Sokolov-Ternov effect [43, 44] was studied e.g. in [33, 34]. An interesting scenario is the impact of particle polarization on the formation of avalanche-type cascades, which may be expected to potentially be a large effect due to its exponential nature.

In this paper, we study the influence of lepton and photon spin and polarization on the formation of QED cascades. We find that the inclusion of particle polarization does affect the growth rates of cascades, and that all particle species in the developing cascades are highly polarized. Moreover, the high-energy tails of the lepton energy spectra are polarized opposite to what is expected from Sokolov-Ternov theory. In photon-seeded cascades we also find an excess of pairs in the early stages when the cascade is seeded by \perp -polarized photons (compared to unpolarized or \parallel -polarized photons), which presents a clear path for robust experimental confirmations of the theoretical results.

Our paper is organized as follows: In Section II we first develop the theoretical model based on a Boltzmann-type kinetic equation with a polarization dependent collision operator. In Section III numerical results are presented and discussed. Our findings are summarized and concluded in Section IV. Technical details and background are provided in the Appendix, including details on the numerical method.

II. THEORETICAL MODEL

So far, in simulations of cascades only the photon polarization was taken into account in [45], but lepton polarization was neglected. That means, in each generation the leptons emit polarized photons, but without any influence from previous generations because leptons are and stay unpolarized. Here, the full polarization evolution is taken into account consistently over many generations. The laser field is described as a rotating electric field $\mathbf{E}(t) = E_0(\cos \omega t, \sin \omega t, 0)$, which is a suitable model for colliding laser pulses widely used in the literature [10, 12, 18, 19, 46–48] and is generated at the magnetic nodes of colliding laser pulses.

We model evolution of the polarized QED cascades by a Boltzmann-type kinetic equation [18, 19, 49, 50] for the one-particle distribution functions f_q^s of of electrons (q = -1), positrons (q = +1) and photons (q = 0), where q is the particle's charge in units of e, and in a polarization state s. At high intensity, $a_0 \gg 1$, the coherence length for the quantum processes λ/a_0 becomes much shorter than the laser wavelength λ [8]. This scale separation allows for Boltzmann type kinetic equations for the evolution of particle distributions with the rates for quantum processes calculated in a constant crossed field. The leptons can be spin-polarized up (\uparrow) or down (\downarrow) along the spin-quantization axis $e_z \parallel E \times p$, which (is the magnetic field direction in the rest frame of the leptons and) does not precess according to the T-BMT equation [33, 51]. In our model the fields are homogeneous so Stern-Gerlach forces are neglected. Further, they can be neglected because they are much weaker than the Lorentz force [34, 40, 52]. Quantum radiation reaction and its spin dependence is included in the calculations automatically through the photon emission. Photons can be in a polarization eigenstate \parallel or \perp to the plane of the rotating electric field. Additional details can be found in Appendix A.

Throughout the paper we use natural Heaviside-Lorentz units with $\hbar = c = \epsilon_0 = 1$. We further introduce normalized (dimensionless) time $\omega t \to t$, momentum $\boldsymbol{p}/m \to \boldsymbol{p}$ and electric field $e\boldsymbol{E}/m\omega \to \boldsymbol{E}$.

The normalized Boltzmann equation can then be written as

$$\left(\frac{\partial}{\partial t} + q\mathbf{E} \cdot \nabla_{\mathbf{p}}\right) f_q^s(\mathbf{p}, t) = \mathcal{C}_q^s[\{f_{q'}^{s'}\}], \qquad (1)$$

where C_q^s are the collision operators describing all relevant strong-field QED processes, with the charge q labelling different particle species. The C_q^s are linear functionals of the spin and polarization dependent differential rates for nonlinear Compton scattering and pair production [8, 45, 53, 54]. The rates were calculated from first-order high-intensity QED Feynman diagrams in the Furry picture within the local constant crossed field approximation [55–57].

The lepton collision operators $\mathcal{C}_{\pm 1}^s$ describe the energy losses due to radiation emission and accompanying spin-flip transitions, as well as a gain term due to pair production by photons. The photon collision operator \mathcal{C}_0^j contains terms for the absorption of j-polarized photons during pair production and the generation of photons by non-linear Compton emission off of electrons and positrons. The explicit expressions for the polarization dependent collision operators are given below in Section II B.

The classical advection operator on the left hand side of Eq. (1) does not mix different polarization states (because of the choice of the non-precessing spin quantization axis, see Appendix A). Only the Boltzmann collision operator on the r.h.s. of Eq. (1) mixes different spin states and, thus, can lead to a change of the polarization of the particles. There is no mixing of different photon polarization states due to vacuum polarization effects since the \parallel / \perp states are eigenstates of the photon polarization tensor [58, 59].

A. Characteristics

The characteristics of the left-hand-side of (1) describing the classical trajectory can be found analytically by solving the equation of motion in the rotating electric field:

$$\mathbf{p}(t) = q \int_{t_0}^t dt' \, \mathbf{E}(t') + \mathbf{p}(t_0) \,, \tag{2}$$

which means $\boldsymbol{p}(t) = (p_x(t), p_y(t), 0)$ lies on a circle with radius a_0 around the center $\boldsymbol{P} = \boldsymbol{p}(t_0) + q\boldsymbol{a}(t_0)$, where $\boldsymbol{a} = -\int \mathrm{d}t\,\boldsymbol{E}$ is the normalized vector potential and \boldsymbol{P} is the conserved canonical momentum. This is just free ballistic motion for the photons, and circular orbits for leptons. Leptons starting with zero momentum can be accelerated up to $p = 2a_0$, where $a_0 = eE_0/m\omega$.

For a numerical solution of the Boltzmann equation it is convenient to transform to a radial coordinate frame co-rotating with the electric field [18]. In the rotating frame, the particle momenta are characterized by their magnitude $p = |\mathbf{p}|$ and by the angle $\varphi = \angle(\mathbf{E}, \mathbf{p})$ with regard to the instantaneous electric field direction. The equations of motion for the

characteristics in the rotating frame coordinates read

$$\frac{\mathrm{d}p}{\mathrm{d}t} = qa_0\cos\varphi\,,\tag{3}$$

$$\frac{\mathrm{d}\varphi}{\mathrm{d}t} = -q\frac{a_0}{p}\sin\varphi - 1\,,\tag{4}$$

with the completely analytical solution,

$$p = \sqrt{p_0^2 + c_0^2 + 2qc_0p_0\cos\left(\varphi_0 - \frac{\Delta t}{2}\right)},$$
 (5)

$$\varphi = \arctan\left(\frac{p_0 \sin \varphi_0 + qc_0 \sin \frac{\Delta t}{2}}{p_0 \cos \varphi_0 + qc_0 \cos \frac{\Delta t}{2}}\right) - \Delta t, \qquad (6)$$

with $c_0 = 2a_0 \sin \frac{\Delta t}{2}$. Here p_0, φ_0 means those quantities are taken at t_0 . The characteristics are written in terms of the time-step $\Delta t = t - t_0$. Note that Eqs. (5) and (6) are exact to all orders in Δt . For the sake of completeness, we also write down the Boltzmann equation in the rotating frame:

$$\left[\frac{\partial}{\partial t} + qa_0 \cos \varphi \frac{\partial}{\partial p} - \left(q \frac{a_0}{p} \sin \varphi + 1\right) \frac{\partial}{\partial \varphi}\right] f_q^s = \mathcal{C}_q^s. \tag{7}$$

B. Polarization dependent collision operators

The benefit of going to the rotating frame becomes apparent when considering the quantum transitions; ultrarelativistic particles emitted during the quantum processes are kinematically restricted to be collinear to the emitting particle and therefore involve transitions at constant φ such that only the magnitude of momentum, p, changes. The angle φ enters the collision operator only parametrically via the quantum parameters

$$\chi_q = \frac{a_0}{a_S} \sqrt{q^2 + p^2 \sin^2 \varphi} \,, \tag{8}$$

which determine the probabilities of the QED processes, and with the normalized Schwinger vector potential $a_S = m/\omega$.

In the rotating frame, quantum transitions leave the angle φ unchanged. This greatly simplifies the numeric calculations. The polarization dependent collision operators for elec-

trons, positrons and photons can be written down as

$$C_{-1}^{s}(p) = -f_{-1}^{s}(p) \sum_{s',j} W_{-1}^{ss'j}(p) + \sum_{j,s'} \int_{p}^{\infty} dp' \frac{p'}{p} f_{-1}^{s'}(p') w_{-1}^{s'sj}(p' \to p) + \sum_{j,s'} \int_{p}^{\infty} dk \frac{k}{p} f_{0}^{j}(k) w_{0}^{s'sj}(k \to k - p),$$

$$(9)$$

$$C_{+1}^{s}(p) = -f_{+1}^{s}(p) \sum_{s',j} W_{+1}^{ss'j}(p) + \sum_{j,s'} \int_{p}^{\infty} dp' \frac{p'}{p} f_{+1}^{s'}(p') w_{+1}^{s'sj}(p' \to p) + \sum_{j,s'} \int_{p}^{\infty} dk \frac{k}{p} f_{0}^{j}(k) w_{0}^{ss'j}(k \to p),$$

$$(10)$$

$$C_0^j(k) = -f_0^j(k) \sum_{s,s'} W_0^{ss'j}(k) + \sum_{q=\pm 1} \sum_{s,s'} \int_k^\infty dp \, \frac{p}{k} f_q^s(p) \, w_q^{ss'j}(p \to p - k)$$
 (11)

The collision operators (9)–(11) are a generalization of both the collision operators to describe the evolution of unpolarized cascades [18, 19, 49, 50], as well as the collision operator for the radiative spin-polarization of electron beams [36]. They are functionals of the differential rates for nonlinear Compton scattering $w_{\pm 1}$ and nonlinear Breit-Wheeler pair production by a photon w_0 , as well as the corresponding total (momentum integrated) rates (see Appendix B for details)

$$W_q^{ss'j}(p) = \int_0^p dk \ w_q^{ss'j}(p \to k) \,,$$
 (12)

as well as the polarized one-particle distribution functions of all particle species f_q^s . We should emphasize again that these collision operators furnish transitions between different momentum of the particles, but only with regard to their magnitude. The angle φ enters only parametrically, and the quantum rates depend on φ only via their respective quantum parameters $\chi_q(p,\varphi)$, Eq. (A4). Let us now briefly discuss the physical meaning of the individual terms in the collision operators.

The first two terms in each of Eqns. (9) and (10) describe the radiative energy loss of the leptons during photon emission, i.e. quantum radiation reaction [19, 60, 61]. These terms include both the possibility of spin-flip and non-flip transitions and thus are also responsible for the radiative lepton polarization, and they had been used already in [36]. In addition, they describe the spin-dependence of quantum radiation reaction. The last term in each of (9) and (10) is for the generation of up/down polarized electrons and positrons from photons of arbitrary polarization, respectively.

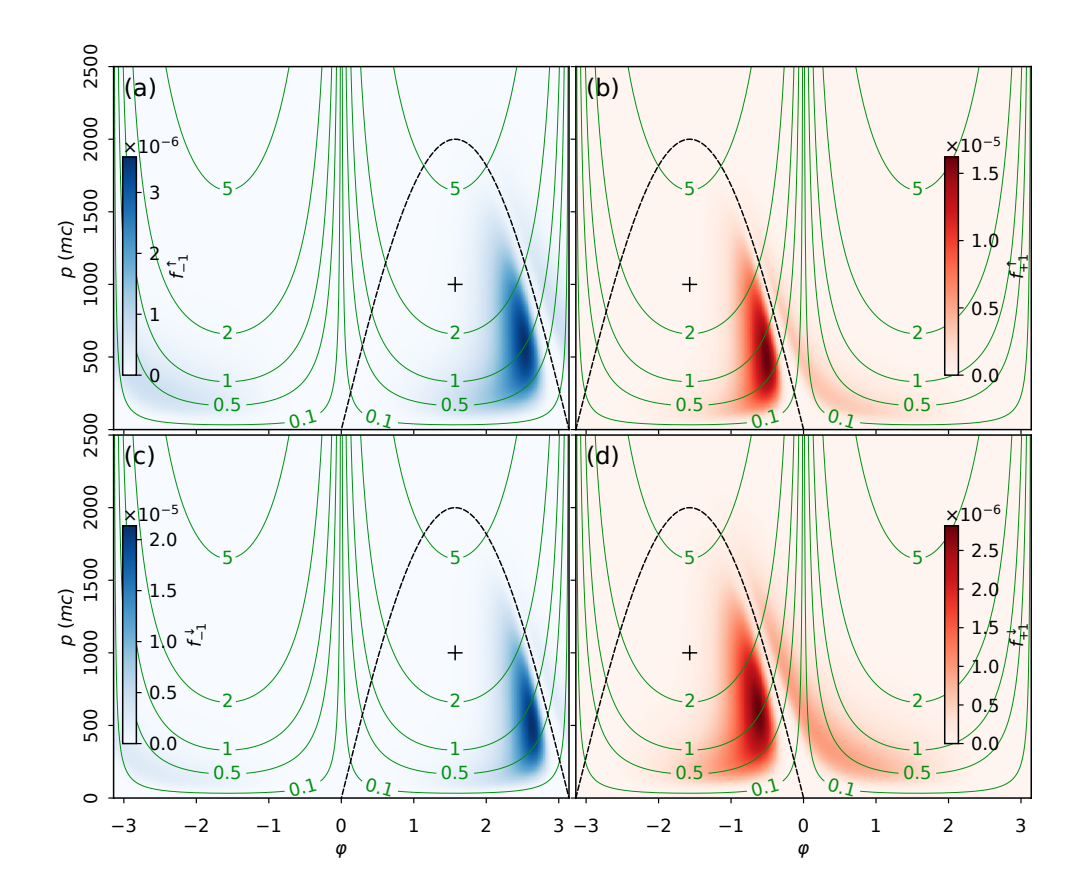


FIG. 1. Snapshot of the electron (a,c) and positron (b,c) distribution functions in an up (a,b) or down (c,d) polarization state for $a_0 = 10^3$ and $\omega t = 10$ in a rotating radial frame. Green curves are χ isocontours. Black dashed curves represent the separatrix of the classical advection $p = -2qa_0 \sin \varphi$, and black crosses are the corresponding fixed points at $(-q\pi/2, a_0)$.

For the photon collision operator $C_0^j(k)$ in Eq. (11) the first term describes the absorption of j-polarized photons during pair production and the second term describes the generation of j-polarized photons by non-linear Compton emission from both electrons and positrons (summed over charge q).

III. RESULTS AND DISCUSSION

Numeric solutions of Eq. (1) for the up and down electron and positron distributions in the presence of both the quantum processes and the classical motion are shown in Fig. 1, for $a_0 = 1000$ and $\omega = 1.55$ eV. In Fig. 1 we also plot the $\chi_{\pm 1}$ isocontours, which greatly vary over the phase space. In particular, at the lines $\varphi = \pm \pi/2$, where the particle momentum and the

electric field are perpendicular, the quantum parameters are $\chi_q \approx a_0 p/a_S$. A characteristic value of χ_q can be defined at the $\mathbf{p} = (a_0, -q\pi/2)$ fixed points of the lepton phase-spaces as $\chi_{\rm FP} \simeq a_0^2/a_S$. For the parameters used in Fig. 1, $\chi_{\rm FP} = 3.03$.

Photons are predominantly generated with \parallel -polarization. Leptons of both polarization states are dominantly produced by photons that reach $\varphi=\pm\pi/2$ because χ_0 is largest there. Leptons produced at $\varphi=q\pi/2$ (i.e. outside the separatrix) are accelerated to large p by the electric field as they orbit to $\varphi=-q\pi/2$ and hence large values of $\chi_{\pm 1}$ exceeding $2a_0^2/a_S$. When $\chi_{\pm 1}\gtrsim 1$, photon emission is efficient, and therefore leptons, while they are being accelerated, are most likely to radiate photons. As a consequence, they lose sufficient energy to enter the closed orbits inside the separatrix, where they accumulate. Note that no classical orbits cross the separatrix and the quantum transitions only take leptons from outside the separatrix to inside, so once inside the separatrix, leptons are trapped. Spin-flip transitions occurring during photon emission lead to further polarization of the leptons. A movie of the evolution of the distribution functions is provided in the supplementary material.

The shape of the distribution and their location inside the separatrix are determined by a balance of classical acceleration, feeding due to pair production, and photon emission. The latter two processes are spin dependent. Therefore, it is not surprising that the shapes of the up and down particle distributions are different. For instance, the values of $\chi_{\pm 1}$ at the maximum of the distributions are 1.04 for up electrons, but only 0.70 for down electrons. The position of the distribution's peak, $\hat{\varphi}$, is also an indicator for the magnitude of radiation reaction effects. In Fig. 1 we find a difference in the angular shift of $\hat{\varphi}_{\downarrow} - \hat{\varphi}_{\uparrow} \simeq 0.1$, signalling a spin-dependence of radiation reaction. By treating radiation reaction semiclassically as a continuous friction force (and neglecting pair production) [62, 63], the angle deviation is proportional to the strength of the radiation reaction force in a lowest order perturbative analysis.

Figure 2 shows the spectra of electrons (a), positrons (b) and photons (c) at $\omega t = 10$ for $a_0 = 1000$, seeded by an unpolarized electron. The plots also show the degree of polarization for each case, i.e. $\int (f_{\pm 1}^{\uparrow} - f_{\pm 1}^{\downarrow}) d\varphi / \int (f_{\pm 1}^{\uparrow} + f_{\pm 1}^{\downarrow}) d\varphi$ for electrons and $\int (f_0^{\parallel} - f_0^{\perp}) d\varphi / \int (f_0^{\parallel} + f_0^{\perp}) d\varphi$ for photons. These plots show that the positron polarization is opposite to the electron polarization. Slight deviations occur because the cascade is seeded by electrons. For the leptons the main peak extends roughly up to $2a_0$, which mostly corresponds to particles accumulating inside the separatrix. Those particles are dominantly polarized, as

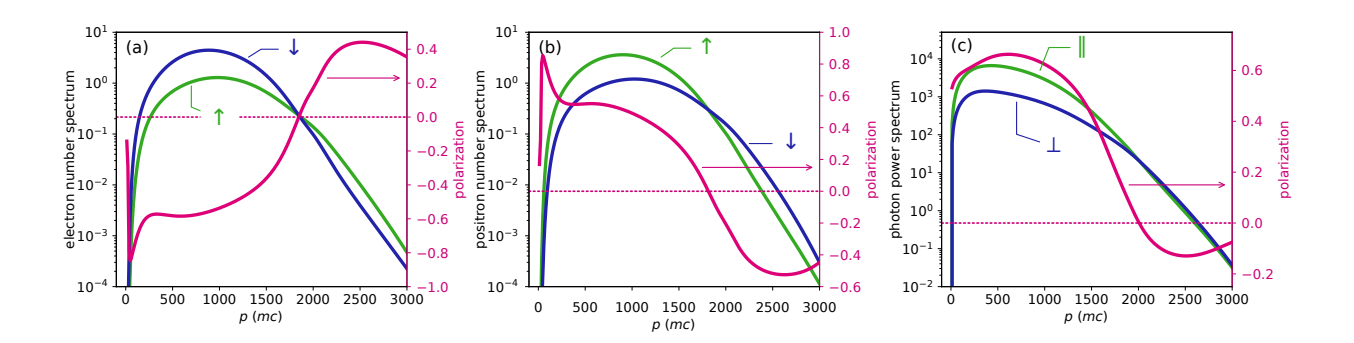


FIG. 2. Momentum spectra (blue / green curves) and differential degree of polarization (pink curve) for electrons (a), positrons (b) and photons (c). Same parameters as in Fig. 1.

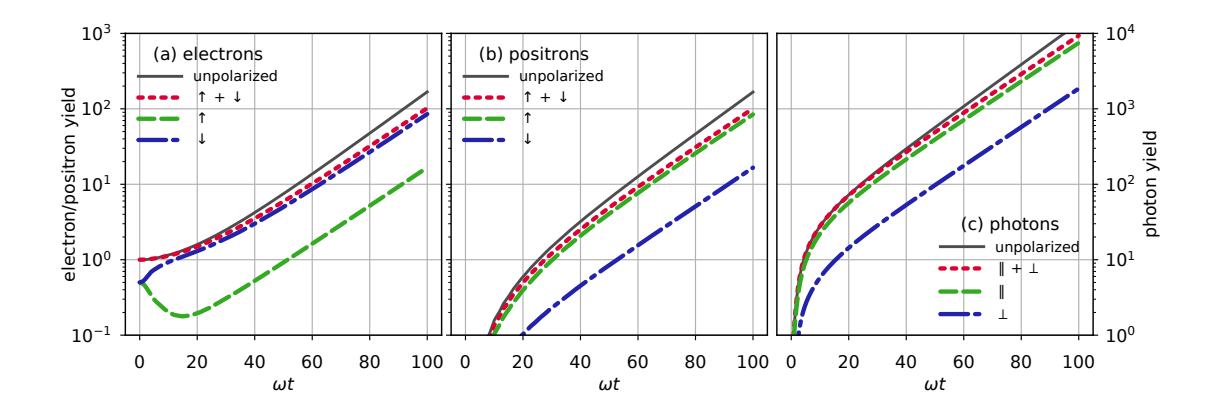


FIG. 3. Time evolution of electron (a), positron (b) and photon (c) yields during a cascade seeded by unpolarized electron, and for $a_0 = 600$ and $\omega = 1.55$ eV. Results for a polarized cascade are compared to an unpolarized cascade simulation.

predicted by Sokolov-Ternov theory, with electrons more likely in a spin-down state (and positrons in an up-state). Interestingly, in the high-energy tail above $p > 2a_0$ —and therefore outside the separatrix—the electrons and positrons are oppositely polarized to the expected Sokolov-Ternov polarization. The reason for this because the highest energy leptons most likely have not emitted a photon since their creation by the decay of a previously generated photon. This effect is "spin-straggling" where one polarization state is more likely to reach the highest values of χ , analogous to straggling effects previously observed without spin [64].

The important findings of previous studies of cascades [10, 12, 18, 19] was that they eventually reach exponential growth in particle number, $n = \int d\varphi dp \, p \, f \propto e^{\Gamma t}$. Our numerically calculated growth rates are in reasonable agreement with the analytical models of [30, 65].

The evolution of the particle yields are shown in Fig. 3 for an unpolarized electron seeded cascade for parameters $a_0 = 600$ and $\omega = 1.55$ eV. We compare a calculation of a polarized cascade with an unpolarized cascade, simulated using only unpolarized distribution functions and rates in the collision operator (see e.g. [18]). Fig. 3 (a) shows that the yields of up electrons decreases initially. This is because of spin flip transitions in the photon emission (Sokolov-Ternov effect). Later in the evolution of the cascade, pair production becomes more relevant and all particle yields enter an exponential growth phase, eventually reaching a common growth rate Γ . In the exponential growth phase there are 5 times more down than up electrons (opposite for positrons). Moreover, a factor of 4 more \parallel -polarized photons are emitted compared to \perp -polarized photons. Thus, the particle distributions produced in a QED cascade are highly polarized.

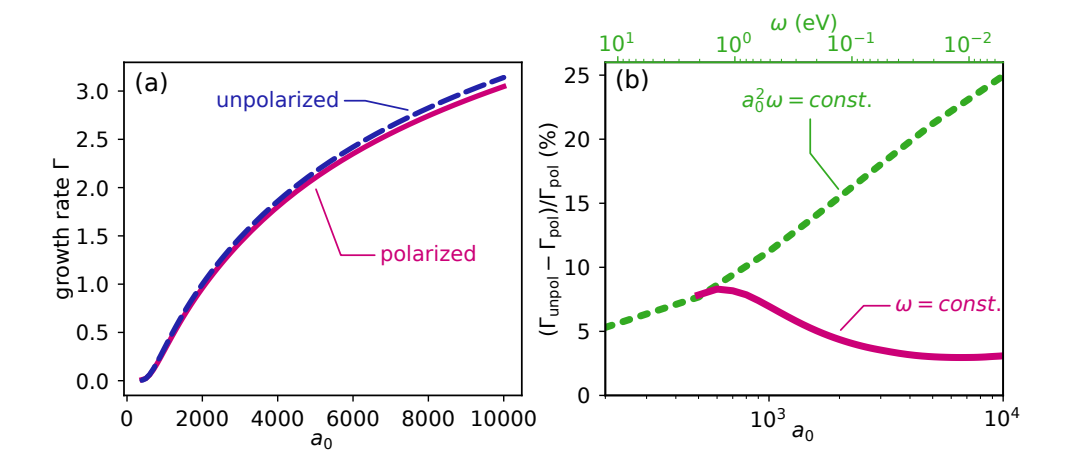


FIG. 4. Cascade growth-rates Γ (a) as a function of a_0 at fixed $\omega = 1.55$ eV and the difference between polarized and unpolarized growth-rates (b) for $\omega = 1.55$ eV = const. (solid) and $\chi_{\text{FP}} = 1 = \text{const.}$ (dashed).

The growth rate is calculated as $\Gamma_q^s = \mathrm{d} \ln n_{qs}/\mathrm{d}t$, with $\Gamma_q^s \to \Gamma$ as $t \to \infty$, and shown as a function of a_0 in Fig. 4 (a). We find that the growth rate of a polarized cascade when electron spin and photon polarization are properly taken into account is typically smaller than in an unpolarized cascade calculation by about 3% to 8%, with the maximum discrepancy around $a_0 = 600$ in this case [red curve in Fig. 4 (b)]. It is worth noting that a reduction in the growth rate of $\sim 5\%$ at a growth rate of ~ 1 (i.e. $a_0 \sim 2000$) corresponds to a reduction in particle yield by an order of magnitude in less than 10 (laser) cycles. For fixed laser frequency ω , the effective value of χ at the fixed point of the classical advection $\chi_{\mathrm{FP}} = a_0^2/a_S$ increases

with a_0 . It is also of interest to examine the behavior at fixed $\chi_{\text{FP}} = a_0^2/a_S = \text{const.} = 1$, which is also shown in Fig. 4 (b). Here, the growth rate differences increase with increasing a_0 and reach 25 % for the longest wavelengths simulated, which is a considerable reduction.

These changes in the growth rates can be traced back to the collision operators for particle species q, summed over all polarization degrees, $C_q \equiv \sum_s C_q^s$. The operators C_q govern the quantum transitions for the distribution function of a particle species summed over all polarization states $f_q = \sum_s f_q^s$. We now isolate the polarization dependent terms in the collision operators C_q and pinpoint the differences to the *unpolarized collision operators* C_0^{unpol} used so far for the description of unpolarized QED cascades.

The unpolarized collision operators C_q^{unpol} contain only the polarization averaged rates of photon emission and pair production,

$$w_q \equiv \frac{1}{2} \sum_{ss'j} w_q^{ss'j} \tag{13}$$

and their momentum-integrated counterparts $W_q = \int_0^k \mathrm{d}p \, w_q(k \to p)$. Until now, only the unpolarized collision operators $\mathcal{C}_q^{\mathrm{unpol}}$ have been used in simulations of QED cascades, see e.g. Refs. [18, 19, 49, 50, 60], but they represent only a part of the full collision operators when the particle polarization is taken into account.

The derivation of the full C_q from the expressions in Eqs. (9)–(11) is lengthy, but straightforward, and the final result reads

$$C_{-1}(p) = C_{-1}^{\text{unpol}}(p) - \Pi_{-1}(p)V_{-1}(p) + \int dk \frac{k}{p} \Pi_{0}(k) v_{0}(k \to p) + \int dk \frac{k}{p} \Pi_{-1}(k) v_{-1}(k \to k - p), \qquad (14)$$

$$C_{+1}(p) = C_{+1}^{\text{unpol}}(p) - \Pi_{+1}(p)V_{+1}(p) + \sum_{q=0,+1} \int dk \frac{k}{p} \Pi_q(k) \, v_q(k \to p)$$
 (15)

$$C_0(k) = C_0^{\text{unpol}}(k) - \Pi_0(k)V_0(k) + \sum_{q=\pm 1} \int dp \frac{p}{k} \Pi_q(p) \, v_q(p \to p - k) \,. \tag{16}$$

We see that the difference between the C_s and the unpolarized collision operators C_0^{unpol} contain terms that couple the polarization imbalances of the lepton, $\Pi_{\pm 1} = f_{\pm 1}^{\uparrow} - f_{\pm 1}^{\downarrow}$, and photon, $\Pi_0 = f_0^{\parallel} - f_0^{\perp}$, distribution functions to the rates' polarization disparities v_q . The latter are defined as the difference of the scattering rates between the initial particle

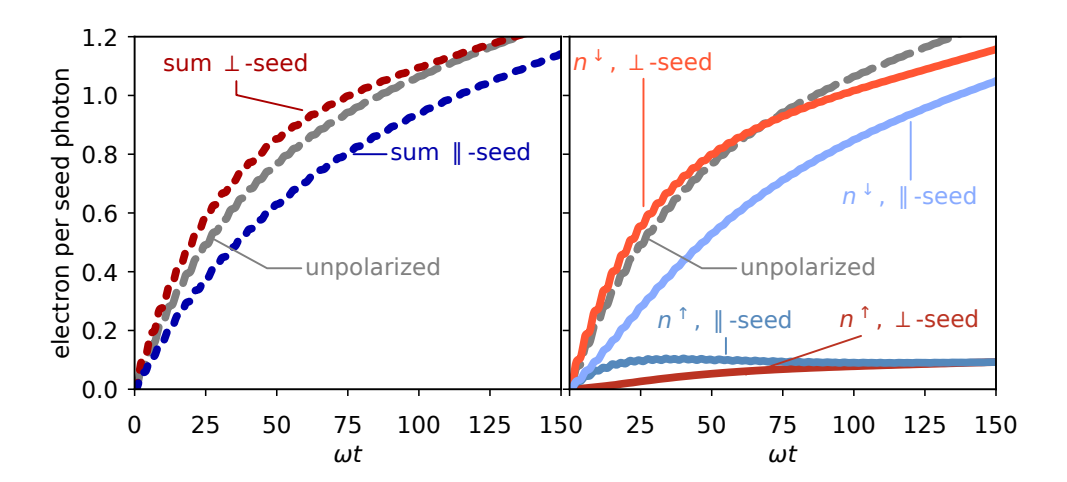


FIG. 5. Time evolution of the electron yield of photon seeded cascade for $a_0 = 400$ and seed photon momentum $k = 10^3 \, mc$, with the seed photon initially either \parallel - or \perp -polarized.

polarizations, summed over all final state polarization

$$v_{\pm 1}(p' \to p) = \frac{1}{2} \sum_{ss'j} s \, w_{\pm 1}^{ss'j}(p' \to p) = \frac{1}{2} \sum_{s'j} \left(w_{\pm 1}^{\uparrow s'j} - w_{\pm 1}^{\downarrow s'j} \right) \,, \tag{17}$$

$$v_0(k \to p) = \frac{1}{2} \sum_{ss'j} j \, w_0^{ss'j}(k \to p) = \frac{1}{2} \sum_{ss'} \left(w_0^{ss'\parallel} - w_0^{ss'\perp} \right) \,, \tag{18}$$

with $s = +1 \Leftrightarrow \uparrow$, $s = -1 \Leftrightarrow \downarrow$, $j = +1 \Leftrightarrow \parallel$, and $j = -1 \Leftrightarrow \bot$. Moreover, we defined the corresponding total rate disparities as, e.g. $V_0(k) = \int dp \, v_0(k \to p)$.

In our model with polarization taken into account, the rate disparities v_q couple to the particle polarizations Π_q , and this affects even the polarization summed collision operators and therefore causes a change in the growth rates.

Seeding for the cascade is an important consideration [30–32]. With the methods developed here, we can also study the evolution of a QED-cascade with an *initially polarized* seed particle distribution to make an experimentally verifiable prediction. We choose to examine a polarized photon seed, since polarized photons could be readily generated and their polarization controlled by inverse Compton scattering [66]. The basic idea could, however, equally work with an initially polarized electron seed.

These calculations were performed with $a_0 = 400$ and a seed photon momentum $k = 10^3 \, mc$, with the seed photon initially either \parallel - or \perp -polarized. Fig. 5 (a) shows the time evolution of the particle yields, depending on the polarization of the seed photons. It shows a significantly higher yield of produced pairs for \perp -polarized seed photons in the early stage.

Moreover, the electron spin distribution depends strongly on the seed photon polarization, see Fig. 5 (b). \perp -polarized photons produce polarized pairs directly, with a very high abundance of down electrons (up positrons). By contrast, \parallel -polarized photons produce equal amounts of up and down electrons and only later are they self-polarized via spin-flip photon emission. For \perp -polarized seeds the yield of down electrons alone exceeds the total electron yield predicted in an unpolarized calculation.

These findings suggest an intriguing experimental scheme to investigate the polarization dependence in strong-field QED-cascades with soon-to-be available lasers: Two counter-propagating, circularly-polarized tightly focused 10 PW laser pulses collide and set up a standing wave. A highly polarized gamma-photon beam is injected into the magnetic nodes of the plane wave where the field is a rotating electric field. Rotating the polarization of the gamma-rays from parallel to perpendicular to the axis of the standing wave will lead to measurable variations in the particle yield, see Fig. 5 (a).

IV. CONCLUSIONS

In conclusion, we have shown that QED-cascades will lead to highly polarized particle generation and that the growth rates are reduced by the spin-dynamics, leading to orders of magnitude differences in particle yield compared with calculations with unpolarized rates under certain conditions. This raises the prospect of generating polarized lepton beam perhaps useful for laser-wakefield driven particle colliders [67], or the production of highly polarized γ -photons [66, 68]. However, addressing the fundamental role of particle polarization in QED cascades, as we have here, could have wide-ranging implications. For example, QED cascades may occur in extreme astrophysical environments such as magnetars and are expected to dominate the behavior of upcoming high intensity laser interactions with matter as intensities increase and we move into the QED-plasma regime. We have shown that polarization dynamics, which is usually neglected, must be included in the modeling of this state. Note that these calculations were performed using an idealised field model, which does not include a magnetic component or the field gradients expected in near-future high-power laser experiments. It is left for further work to explore the impacts of these effects on the interaction.

This work supported by the US ARO Grant no. W911NF-16-1-0044, AFOSR Grant No. FA9550-16-1-0121, NSF grant 1804463 and UK Engineering and Physical Sciences Research Council grant EP/M018156/1. D.S. acknowledges valuable discussions with Ben King and Felix Karbstein.

Appendix A: Boltzmann Equation

The kinetic equation for the one-particle distribution functions of relativistic spin-1/2 particles has been derived in [52] [see Eq. (12) therein] and reads

$$\left(\frac{\partial}{\partial t} + \frac{\mathbf{p}}{\varepsilon} \cdot \nabla_{\mathbf{x}} + qe(\mathbf{E} + \frac{\mathbf{p}}{\varepsilon} \times \mathbf{B}) \cdot \nabla_{\mathbf{p}} + \frac{2\mu_{B}m}{\varepsilon} \left[\mathbf{s} \times \left(\mathbf{B} - \frac{\mathbf{p} \times \mathbf{E}}{\varepsilon + m} \right) \right] \cdot \nabla_{\mathbf{s}} + [\dots] \right) f(\mathbf{x}, \mathbf{p}, \mathbf{s}, t) = 0, \quad (A1)$$

where $f(\boldsymbol{x},\boldsymbol{p},\boldsymbol{s},t)$ is the probability to measure the electron with spin-up in the direction $\boldsymbol{s}.\ \varepsilon=\sqrt{m^2+\boldsymbol{p}^2}$ is the particle energy. The [...] stands for extra terms that contain field gradients and other spin-dependent terms which are not relevant for our case of a rotating electric field. The above equation describes the quasi-classical evolution of the one-particle lepton distribution functions in an extended phase space [52]. In our work, the f_q^s are the one-particle distribution functions of a particle with charge q in a discrete polarization state s. They are related to the distribution $f(\boldsymbol{p},\boldsymbol{s},t)$ in extended phase space by integrating over spin-space \boldsymbol{s} for a distribution in a given pure up or down spin-state relative to some axis. For electrons circulating in a rotating electric field $\boldsymbol{E}=E_0(\cos\omega t,\sin\omega t,0)$ and $\boldsymbol{B}=0$ we can choose the spin-axis parallel to the z-axis, \boldsymbol{e}_z , such that on integrating Eq. (A1), the term $\boldsymbol{s}\times(\boldsymbol{p}\times\boldsymbol{E})\cdot\nabla_s f$ drops out.

Quantum transitions are included by a Boltzmann-type collision operator C_q^s . If we use the charge q to distinguish the different particle species—electrons (q = -1), positrons (q = +1) and including photons (q = -0)—the Boltzmann equation can be compactly written as

$$\left(\frac{\partial}{\partial t} + qe\mathbf{E} \cdot \nabla_{\mathbf{p}}\right) f_q^s = \mathcal{C}_q^s[\{f_{q'}^{s'}\}]. \tag{A2}$$

These are in total 6 equations for the coupled electron-positron-photon system with all spin and polarization states are taken into account. The collision operators C_q^s describe all relevant strong-field QED effects for polarized particles, and possible transitions between

those polarized particle species: polarized photon emission by polarized leptons and pair production by polarized photons. It is a linear functional of the corresponding quantum probability rates and the particle distribution functions.

The two independent polarization states for electrons (and positrons) are $s=\uparrow$ and $s=\downarrow$ where the spin is aligned (anti-aligned) to the axis e_z [33] as discussed above. For photons, the two independent polarization states are $s=\bot$ (polarization vector perpendicular to the plane of \mathbf{E}) and $s=\parallel$ (polarization vector lies in the plane in which \mathbf{E} rotates). The polarization four-vectors associated to those polarization states are $\Lambda^{\mu}_{\parallel} = F^{\mu\nu}k_{\nu}/||F^{\mu\nu}k_{\nu}||$ and $\Lambda^{\mu}_{\perp} = \tilde{F}^{\mu\nu}k_{\nu}/||\tilde{F}^{\mu\nu}k_{\nu}||$, which are by construction transverse to the photon four-momentum k^{μ} , i.e. $\Lambda^{\mu}_{s}k_{\mu} = 0$ [69]. $\tilde{F}^{\mu\nu}$ is the dual electromagnetic field strength tensor.

Following from the discussion of the general spin-1/2 kinetic equation above, the classical advection operator on the left hand side of (A2) [and Eq. (1)] is independent of the particle spin, and does not mix different spin states. Polarized leptons are produced by the collision operators with their spins aligned to the global non-precessing spin quantization axis e_z . Thus, the spins of the produced leptons do not precess according to the T-BMT equation [51] in the rotating electric field configuration. Moreover, as was discussed above, spin-gradient forces can be neglected because (i) in our model the fields are homogeneous and (ii) Stern-Gerlach forces are much weaker than the Lorentz force [34, 40].

The transition rates in the collision operator are all functions of their respective quantum parameter

$$\chi_q = \frac{e}{m^3} \sqrt{\varepsilon^2 \mathbf{E}^2 - (\mathbf{p} \cdot \mathbf{E})^2}, \qquad (A3)$$

In the normalized units this can be written as

$$\chi_q = \frac{a_0}{a_S} \sqrt{q^2 + p^2 \sin^2 \varphi} \,, \tag{A4}$$

where $\varphi = \angle(\boldsymbol{E}, \boldsymbol{p})$ is the angle between the particle momentum and the instantaneous direction of the electric field vector, and $q = 0, \pm 1$ is the charge labelling the different particle species. Here we have introduced the dimensionless vector potential $a_0 = (E_0/E_S)a_S$, where $E_S = m^2/e$ is the Sauter-Schwinger field and $a_S = m/\omega$.

Appendix B: Completely Polarized Rates for Quantum Processes

Here we provide the full analytic expressions for the fully polarized rates of photon emission and pair production that enter the collision operator (9)–(11). The rates noted here are the probabilities for the process to happen per unit normalized time ωt .

The fully polarized differential photon emission probability for an electron with normalized momentum p to emit a photon with momentum k, and go to a momentum state p' = p - k is given by

$$w_{-1}^{ss'j}(p \to p') = -\frac{\alpha a_S}{4p\sqrt{1+p^2}} \left[\left\{ 1 + ss' + jss'(1-g) \right\} \operatorname{Ai}_1(z) + \left\{ ys + us' + j(us + ys') \right\} \frac{\operatorname{Ai}(z)}{\sqrt{z}} + \left\{ g + ss' + j\frac{1+gss'}{2} \right\} \frac{2\operatorname{Ai}'(z)}{z} \right], \quad (B1)$$

where y=k/p=1-p'/p, u=y/(1-y), g=1+uy/2. Ai is the Airy function with argument $z=(u/\chi_{-1})^{2/3}$, Ai' its derivative and Ai₁ the integral Ai₁(z) = $\int_z^\infty \mathrm{d}x \, \mathrm{Ai}(x)$. j is the photon polarization index, j=+1 for the \parallel state and j=-1 for the \perp state. For the electron spin-states s=+1 for up electrons and s=-1 for down electrons. For instance, $w_{-1}^{\uparrow\downarrow\perp}$ is the probability rate that an up electron emits a photon that is polarized perpendicularly to the electric field in a spin-flip transition going to a spin down state. The rates for positrons emitting photons in Eq. (10) can be obtained from the electron rates by inverting all lepton spin variables, $w_{+1}^{ss'j}(p\to p')=w_{-1}^{\bar{s}\bar{s}'j}(p\to p')$.

The rates for the non-linear Breit-Wheeler pair production by a high-energy photon with momentum k in a polarization state j are given by

$$w_0^{ss'j}(k \to p) = \frac{\alpha a_S}{4k^2} \left[\left\{ 1 + ss' + jss'(1 - \tilde{g}) \right\} \operatorname{Ai}_1(\tilde{z}) + \left\{ \frac{s}{r} - \frac{s'}{1 - r} + j \left(\frac{s'}{r} - \frac{s}{1 - r} \right) \right\} \frac{\operatorname{Ai}(\tilde{z})}{\sqrt{\tilde{z}}} + \left\{ (\tilde{g} + ss') + j \frac{1 + \tilde{g}ss'}{2} \right\} \frac{2\operatorname{Ai}'(\tilde{z})}{\tilde{z}} \right], \quad (B2)$$

with the Airy function argument $\tilde{z}=\left(\frac{1}{\chi_0 r(1-r)}\right)^{2/3}$, $\tilde{g}=1-\frac{1}{2r(1-r)}$, with r=p/k with p being the generated positron momentum and p' the electron momentum. The approximate momentum conservation now reads k=p+p'. Here, $s=\pm 1$ is the positron spin and $s'=\pm 1$ the electron spin.

These spin and polarization dependent rates are derived from strong-field QED process in a general plane-wave laser pulse in the Furry picture by applying the local constant field

approximation (LCFA) [57]. The LCFA generally is considered a good approximation of the full strong-field QED processes if the formation length for the emission of the photon λ/a_0 is short compared to λ . This is usually the case for $a_0 \gg 1$, but additional constraints, e.g. $a_0^3/\chi \gg 1$ are required [70]. Moreover, it is known that the LCFA can break down for the emission of low-energy photons as for those the coherence length for the formation of the process is $\sim \lambda$ even for $a_0 \gg 1$. The assumption of localized emission is accurate for the emission high-energy photons with energies $k/p \gtrsim \chi/a_0^3$ [55, 56]. Low-energy photons violating that condition are not of high relevance for the formation of cascades since (i) electrons emitting soft photons lose only very little energy and thus radiation reaction effects are described with reasonable accuracy within the LCFA even though the photon number spectrum might not be correct at very low k; (ii) low-energy photons cannot produce pairs for subsequent generations of cascade particles and thus are expected to affect the growth rates only weakly at most. In addition, collinear emission can be assumed for ultrarelativistic particles with $\gamma \gg 1$ (see also [56] for a discussion non-collinearity effects and its energy dependence). Strictly speaking, the momentum conservation laws found from analysing the strong-field QED S-matrix elements for the scattering in a plane wave background with four-wavevector κ^{μ} are exact for three light-front components of the respective momenta, $\kappa.p' = \kappa.p + \kappa.k$ and $p'^{\perp} = k^{\perp} + p^{\perp}$. In the ultra-relativistic scattering case energy and linear momentum are typically conserved up to terms of the order $1/\gamma \ll 1$, and the LCFA rates may be used for ultrarelativistic particles interacting with an arbitrary field since in the particle's rest frame the field is boosted to look almost exactly like a crossed field.

Appendix C: Numerical Methods

The Boltzmann-type kinetic equations are solved numerically on a rotating radial momentum-space mesh, with typically 300×400 grid points both p and φ . The time-evolution is calculated using a time-centered operator-splitting method. A time-step of $\Delta t = 0.005$ is used for all simulations presented in the main text. Numerical convergence of the momentum space discretization and the time step was verified.

To solve the classical advection in the rotating frame we use a semi-lagrangian algorithm which is very efficient, because the characteristics are known analytically, Eqs. (5) and (6), and the distribution functions f_q^s are constant along the characteristics. For each grid point

of discretized momentum space (p_n, φ_k) we employ the characteristics Eqns. (5) and (6) in order to determine the origin (p'_n, φ'_k) of the parcel at time $t - \Delta t$ arriving at (p_n, φ_k) at time t. The distribution functions are interpolated onto (p'_n, φ'_k) using bi-cubic splines, where the periodicity in φ is ensured.

The action of the collision operator onto the discretized distribution functions can be described by matrix multiplications after discretizing p onto the co-rotating radial grid (p_n, φ_k) . Those matrices act only on the magnitude p_n ; the angle φ_k appears only parametrically via the quantum parameters χ_q . Thus, independently for each value of φ_k we have $\Delta f_q^s(p_m) = (\mathcal{C}_q^s(p_m))_{\text{discr}} \Delta t = \sum_{n,q',s'} (M_{qq'}^{ss'})_{mn} f_{q'}^{s'}(p_n) \Delta t$. For instance, the matrix for electron spin-flip from down to up during photon-emission and the up-up non-flip tansition are given by

$$(M_{-1,-1}^{\uparrow\downarrow})_{mn} = \sum_{j} \Delta p \frac{p_n}{p_m} w_{-1}^{\downarrow\uparrow j}(p_n \to p_m)$$
 (C1)

$$(M_{-1,-1}^{\uparrow\uparrow})_{mn} = \sum_{j} \Delta p \frac{p_n}{p_m} w_{-1}^{\uparrow\uparrow j}(p_n \to p_m) - \delta_{mn} \Delta p \sum_{s',j} \sum_{k \le n} w_{-1}^{\uparrow s'j}(p_n \to p_k), \qquad (C2)$$

for $n \geq m$, and zero otherwise. For more details on the discretization of the collision operator see for instance Ref. [71]. Our numerical scheme is charge conserving, i.e. the total charge $Q = \sum_{s,q} q \int \mathrm{d}p \mathrm{d}\varphi \, p \, f_q^s = const.$

As initial distributions for calculations of electron seeded cascades we used the identical distributions for up and down electrons, $f_{-1}^{\uparrow}(p,\varphi,t=0) = f_{-1}^{\downarrow}(p,\varphi,t=0) = \mathcal{N} \times e^{-p^2/2w^2}$, where the normalization constant \mathcal{N} is chosen such that the initial distributions are each normalized to 1/2. We did run simulations with width w=100 and $w=a_0/4$, with almost negligible differences in the cascade evolution. For photon seeded cascades the initial distributions are $f_0^j(k,\varphi,t=0) = \mathcal{N}e^{-(k-k_0)^2/2w^2}e^{-4\varphi^2}$, normalized to 1, for either $j=\parallel$ or $j=\perp$, and with $k_0=1000$ and w=100.

^[1] C. N. Danson, C. Haefner, J. Bromage, T. Butcher, J.-C. F. Chanteloup, E. A. Chowdhury, A. Galvanauskas, L. A. Gizzi, J. Hein, D. I. Hillier, N. W. Hopps, Y. Kato, E. A. Khazanov, R. Kodama, G. Korn, R. Li, Y. Li, J. Limpert, J. Ma, C. H. Nam, D. Neely, D. Papadopoulos, R. R. Penman, L. Qian, J. J. Rocca, A. A. Shaykin, C. W. Siders, C. Spindloe, S. Szatmári,

- R. M. G. M. Trines, J. Zhu, P. Zhu, and J. D. Zuegel, "Petawatt and exawatt class lasers worldwide," High Power Laser Sci. Eng. 7, e54 (2019).
- [2] J. M. Cole, K. T. Behm, E. Gerstmayr, T. G. Blackburn, J. C. Wood, C. D. Baird, M. J. Duff, C. Harvey, A. Ilderton, A. S. Joglekar, K. Krushelnick, S. Kuschel, M. Marklund, P. McKenna, C. D. Murphy, K. Poder, C. P. Ridgers, G. M. Samarin, G. Sarri, D. R. Symes, A. G. R. Thomas, J. Warwick, M. Zepf, Z. Najmudin, and S. P. D. Mangles, "Experimental Evidence of Radiation Reaction in the Collision of a High-Intensity Laser Pulse with a Laser-Wakefield Accelerated Electron Beam," Phys. Rev. X 8, 011020 (2018), arXiv:1707.06821.
- [3] K. Poder, M. Tamburini, G. Sarri, A. Di Piazza, S. Kuschel, C. D. Baird, K. Behm, S. Bohlen, J. M. Cole, D. J. Corvan, M. Duff, E. Gerstmayr, C. H. Keitel, K. Krushelnick, S. P. D. Mangles, P. McKenna, C. D. Murphy, Z. Najmudin, C. P. Ridgers, G. M. Samarin, D. R. Symes, A. G. R. Thomas, J. Warwick, and M. Zepf, "Experimental Signatures of the Quantum Nature of Radiation Reaction in the Field of an Ultraintense Laser," Phys. Rev. X 8, 031004 (2018), arXiv:1709.01861.
- [4] T. G. Blackburn, "Radiation reaction in electron-beam interactions with high-intensity lasers," Rev. Mod. Plasma Phys. 4, 5 (2020), arXiv:1910.13377.
- [5] K. A. Tanaka, K. M. Spohr, D. L. Balabanski, S. Balascuta, L. Capponi, M. O. Cernaianu, M. Cuciuc, A. Cucoanes, I. Dancus, A. Dhal, B. Diaconescu, D. Doria, P. Ghenuche, D. G. Ghita, S. Kisyov, V. Nastasa, J. F. Ong, F. Rotaru, D. Sangwan, P.-A. Söderström, D. Stutman, G. Suliman, O. Tesileanu, L. Tudor, N. Tsoneva, C. A. Ur, D. Ursescu, and N. V. Zamfir, "Current status and highlights of the ELI-NP research program," Matter Radiat. Extrem. 5, 024402 (2020).
- [6] E. Cartlidge, "The light fantastic," Science **359**, 382–385 (2018).
- [7] P. Zhang, S. S. Bulanov, D. Seipt, A. V. Arefiev, and A. G. R. Thomas, "Relativistic Plasma Physics in Supercritical Fields," Phys. Plasmas 27, 050601 (2020), arXiv:2001.00957.
- [8] V. I. Ritus, "Quantum effects of the interaction of elementary particles with an intense electromagnetic field," J. Sov. Laser Res. 6, 497 (1985).
- [9] A. Di Piazza, C. Müller, K. Z. Hatsagortsyan, and C. H. Keitel, "Extremely high-intensity laser interactions with fundamental quantum systems," Rev. Mod. Phys. 84, 1177–1228 (2012).
- [10] A. R. Bell and J G. Kirk, "Possibility of prolific pair production with high-power lasers." Phys. Rev. Lett. 101, 200403 (2008).

- [11] This corresponds to a laser intensity of $I_S = 4 \times 10^{29} \text{ W/cm}^2$ for a wavelength of 800 nm.
- [12] A. M. Fedotov, N. B. Narozhny, G. Mourou, and G. Korn, "Limitations on the Attainable Intensity of High Power Lasers," Phys. Rev. Lett. 105, 080402 (2010).
- [13] T. Grismayer, M. Vranic, J. L. Martins, R. A. Fonseca, and L. O. Silva, "Laser absorption via quantum electrodynamics cascades in counter propagating laser pulses," Phys. Plasmas 23, 056706 (2016).
- [14] D. Seipt, T. Heinzl, M. Marklund, and S.S. Bulanov, "Depletion of Intense Fields," Phys. Rev. Lett. 118, 154803 (2017).
- [15] J. G. Kirk, A. R. Bell, and I. Arka, "Pair production in counter-propagating laser beams," Plasma Phys. Control. Fusion **51**, 085008 (2009).
- [16] S. S. Bulanov, T. Zh. Esirkepov, A. G. R. Thomas, J. K. Koga, and S. V. Bulanov, "Schwinger Limit Attainability with Extreme Power Lasers," Phys. Rev. Lett. 105, 220407 (2010).
- [17] E. N. Nerush, I. Yu. Kostyukov, A. M. Fedotov, N. B. Narozhny, N. V. Elkina, and H. Ruhl, "Laser Field Absorption in Self-Generated Electron-Positron Pair Plasma," Phys. Rev. Lett. 106, 035001 (2011).
- [18] E. N. Nerush, V. F. Bashmakov, and I. Yu. Kostyukov, "Analytical model for electromagnetic cascades in rotating electric field," Phys. Plasmas 18, 83107 (2011).
- [19] N. V. Elkina, A. M. Fedotov, I. Yu. Kostyukov, M. V. Legkov, N. B. Narozhny, E. N. Nerush, and H. Ruhl, "QED cascades induced by circularly polarized laser fields," Phys. Rev. Spec. Top. Accel. Beams 14, 054401 (2011).
- [20] C. Slade-Lowther, D. Del Sorbo, and C. P. Ridgers, "Identifying the electron-positron cascade regimes in high-intensity laser-matter interactions," New J. Phys. 21, 013028 (2019).
- [21] C. Bamber, S. J. Boege, T. Koffas, T. Kotseroglou, A. C. Melissinos, D. D. Meyerhofer, D. A. Reis, W. Ragg, C. Bula, K. T. McDonald, E. J. Prebys, D. L. Burke, R. C. Field, G. Horton-Smith, J. E. Spencer, D. Walz, S. C. Berridge, W. M. Bugg, K. Shmakov, and A. W. Weidemann, "Studies of nonlinear QED in collisions of 46.6 GeV electrons with intense laser pulses," Phys. Rev. D 60, 092004 (1999).
- [22] H. Abramowicz, M. Altarelli, R. Aßmann, T. Behnke, Y. Benhammou, O. Borysov, M. Borysova, R. Brinkmann, F. Burkart, K. Büßer, O. Davidi, W. Decking, N. Elkina, H. Harsh, A. Hartin, I. Hartl, B. Heinemann, T. Heinzl, N. TalHod, M. Hoffmann, A. Ilderton, B. King, A. Levy, J. List, A. R. Maier, E. Negodin, G. Perez, I. Pomerantz, A. Ringwald, C. Rödel,

- M. Saimpert, F. Salgado, G. Sarri, I. Savoray, T. Teter, M. Wing, and M. Zepf, "Letter of Intent for the LUXE Experiment," (2019), arXiv:1909.00860.
- [23] S. Meuren, P. H. Bucksbaum, N. J. Fisch, F. Fiúza, S. Glenzer, M. J. Hogan, K. Qu, D. A. Reis, G. White, and V. Yakimenko, "On Seminal HEDP Research Opportunities Enabled by Colocating Multi-Petawatt Laser with High-Density Electron Beams,", 1–11 (2020), arXiv:2002.10051.
- [24] F.A. Aharonian and A.V. Plyasheshnikov, "Similarities and differences between relativistic electron-photon cascades developed in matter, photon gas and magnetic field," Astropart. Phys. 19, 525–548 (2003).
- [25] P. A. Sturrock, "A Model of Pulsars," Astrophys. J. 164, 529 (1971).
- [26] M. A. Ruderman and P. G. Sutherland, "Theory of pulsars Polar caps, sparks, and coherent microwave radiation," Astrophys. J. 196, 51 (1975).
- [27] C. P. Ridgers, J. G. Kirk, R. Duclous, T. G. Blackburn, C. S. Brady, K. Bennett, T. D. Arber, and A. R. Bell, "Modelling gamma-ray photon emission and pair production in high-intensity laser-matter interactions," J. Comput. Phys. 260, 273–285 (2014), arXiv:1311.5551.
- [28] V. F. Bashmakov, E. N. Nerush, I. Yu Kostyukov, A. M. Fedotov, and N. B. Narozhny, "Effect of laser polarization on quantum electrodynamical cascading," Phys. Plasmas 21 (2014), 10.1063/1.4861863.
- [29] T. Zh. Esirkepov, S. S. Bulanov, J. K. Koga, M. Kando, K. Kondo, N. N. Rosanov, G. Korn, and S. V. Bulanov, "Attractors and chaos of electron dynamics in electromagnetic standing waves," Phys. Lett. A 379, 2044–2054 (2015), arXiv:1412.6028.
- [30] T. Grismayer, M. Vranic, J. L. Martins, R. A. Fonseca, and L. O. Silva, "Seeded qed cascades in counter propagating laser pulses," Phys. Rev. E 95, 023210 (2017).
- [31] M. Jirka, O. Klimo, S. V. Bulanov, T. Z. Esirkepov, E. Gelfer, S. S. Bulanov, S. Weber, , and G. Korn, "Electron dynamics and gamma and e-p production by colliding laser pulses," Phys. Rev. E 93, 023207 (2016).
- [32] M. Tamburini, A. Di Piazza, and C. H. Keitel, "Laser-pulse-shape control of seeded QED cascades," Sci. Rep. 7, 5694 (2017).
- [33] D. Del Sorbo, D. Seipt, T. G. Blackburn, A. G. R. Thomas, C. D. Murphy, J. G. Kirk, and C. P. Ridgers, "Spin polarization of electrons by ultraintense lasers," Phys. Rev. A 96, 043407 (2017).

- [34] D. Del Sorbo, D. Seipt, A. G. R. Thomas, and C. P. Ridgers, "Electron spin polarization in realistic trajectories around the magnetic node of two counter-propagating, circularly polarized, ultra-intense lasers," Plasma Phys. Control. Fusion 60, 064003 (2018), arXiv:1712.08118.
- [35] D. Seipt, D. Del Sorbo, C. P. Ridgers, and A. G. R. Thomas, "Theory of radiative electron polarization in strong laser fields," Phys. Rev. A 98, 023417 (2018).
- [36] D. Seipt, D. Del Sorbo, C. P. Ridgers, and A. G. R. Thomas, "Ultrafast polarization of an electron beam in an intense bichromatic laser field," Phys. Rev. A 100, 061402 (2019), arXiv:1904.12037.
- [37] Y.-F. Li, R. Shaisultanov, K. Z. Hatsagortsyan, F. Wan, C. H. Keitel, and J.-X. Li, "Ultra-relativistic Electron-Beam Polarization in Single-Shot Interaction with an Ultraintense Laser Pulse," Phys. Rev. Lett. 122, 154801 (2019), arXiv:1812.07229.
- [38] Y.-Y. Chen, P.-L. He, R. Shaisultanov, K. Z. Hatsagortsyan, and C. H. Keitel, "Polarized Positron Beams via Intense Two-Color Laser Pulses," Phys. Rev. Lett. 123, 174801 (2019), arXiv:1904.04110.
- [39] F. Wan, R. Shaisultanov, Y.-F. Li, K. Z. Hatsagortsyan, C. H. Keitel, and J.-X. Li, "Ultrarel-ativistic polarized positron jets via collision of electron and ultraintense laser beams," Phys. Lett. B 800, 135120 (2020), arXiv:1904.04305.
- [40] J. Thomas, A. Hützen, A. Lehrach, A. Pukhov, L. Ji, Y. Wu, X. Geng, and M. Büscher, "Scaling laws for the (de-)polarization time of relativistic particle beams in strong fields,", 1–17 (2020), arXiv:2001.07084.
- [41] D. Yu. Ivanov, G. L. Kotkin, and V. G. Serbo, "Complete description of polarization effects in emission of a photon by an electron in the field of a strong laser wave," Eur. Phys. J. C 36, 127–145 (2004).
- [42] D. Yu. Ivanov, G. L. Kotkin, and V. G. Serbo, "Complete description of polarization effects in e^+e^- pair production by a photon in the field of a strong laser wave," Eur. Phys. J. C 40, 27 (2005).
- [43] A. A. Sokolov and I. M. Ternov, Synchrotron Radiation (Akademie Verlag, Berlin, 1968).
- [44] I. M. Ternov, "Synchrotron Radiation," Phys. Usp. 38, 409–434 (1995).
- [45] B. King, N. Elkina, and H. Ruhl, "Photon polarization in electron-seeded pair-creation cascades," Phys. Rev. A 87, 042117 (2013).
- [46] A. Blinne and H. Gies, "Pair production in rotating electric fields," Phys. Rev. D 89, 085001

(2014).

- [47] A. A. Mironov, N. B. Narozhny, and A. M. Fedotov, "Collapse and revival of electromagnetic cascades in focused intense laser pulses," Phys. Lett. Sect. A Gen. At. Solid State Phys. 378, 3254–3257 (2014).
- [48] Christian Kohlfürst, "Spin states in multiphoton pair production for circularly polarized light," Phys. Rev. D **99**, 096017 (2019), arXiv:arXiv:1812.03130v1.
- [49] N. Neitz and A. Di Piazza, "Stochasticity Effects in Quantum Radiation Reaction," Phys. Rev. Lett. 111, 054802 (2013).
- [50] S. S. Bulanov, C. B. Schroeder, E. Esarey, and W. P. Leemans, "Electromagnetic cascade in high-energy electron, positron, and photon interactions with intense laser pulses," Phys. Rev. A 87, 062110 (2013).
- [51] V. Bargmann, L. Michel, and V. L. Telegdi, "Precession of the Polarization of Particles Moving in a Homogeneous Electromagnetic Field," Phys. Rev. Lett. 2, 435–436 (1959).
- [52] R. Ekman, F. A. Asenjo, and J. Zamanian, "Relativistic kinetic equation for spin-1/2 particles in the long-scale-length approximation," Phys. Rev. E 96, 023207 (2017), arXiv:1702.00722.
- [53] A. I. Nikishov and V. I. Ritus, "Quantum processes in the field of a plane electromagnetic wave and in a constant field," Sov. Phys. J. Exp. Theor. Phys. 19, 1191 (1964).
- [54] D. Seipt and B. Kämpfer, "Non-Linear Compton Scattering of Ultrashort and Intense Laser Pulses," Phys. Rev. A 83, 022101 (2011).
- [55] A Ilderton, B King, and D Seipt, "Extended locally constant field approximation for nonlinear Compton scattering," Phys. Rev. A 99, 042121 (2019).
- [56] T. G. Blackburn, D. Seipt, S. S. Bulanov, and M. Marklund, "Radiation beaming in the quantum regime," Phys. Rev. A 101, 012505 (2020), arXiv:1904.07745.
- [57] D. Seipt and B. King, "Spin and polarisation dependent LCFA rates for nonlinear Compton and Breit-Wheeler processes," Phys. Rev. A in production (2020), arXiv:2007.11837 [physics.plasm-ph].
- [58] F. Karbstein, "Photon polarization tensor in a homogeneous magnetic or electric field," Phys. Rev. D 88, 085033 (2013), arXiv:1308.6184.
- [59] B. King and N. Elkina, "Vacuum birefringence in high-energy laser-electron collisions," Phys. Rev. A 94, 062102 (2016), arXiv:1603.06946.
- [60] F. Niel, C. Riconda, F. Amiranoff, R. Duclous, and M. Grech, "From quantum to classical

- modeling of radiation reaction: A focus on stochasticity effects," Phys. Rev. E **97**, 043209 (2018), arXiv:1707.02618.
- [61] C. P. Ridgers, T. G. Blackburn, D. Del Sorbo, L. E. Bradley, C. Slade-Lowther, C. D. Baird, S. P. D. Mangles, P. McKenna, M. Marklund, C. D. Murphy, and A. G. R. Thomas, "Signatures of quantum effects on radiation reaction in laser-electron-beam collisions," J. Plasma Phys. 83, 715830502 (2017), arXiv:1708.04511.
- [62] S. V. Bulanov, T. Zh. Esirkepov, M. Kando, J. K. Koga, and S. S. Bulanov, "Lorentz-Abraham-Dirac versus Landau-Lifshitz radiation friction force in the ultrarelativistic electron interaction with electromagnetic wave (exact solutions)," Phys. Rev. E 84, 056605 (2011).
- [63] P. Zhang, C. P. Ridgers, and A. G. R. Thomas, "The effect of nonlinear quantum electrodynamics on relativistic transparency and laser absorption in ultra-relativistic plasmas," New J. Phys. 17, 043051 (2015), arXiv:arXiv:1403.5034.
- [64] T. G. Blackburn, C. P. Ridgers, J. G. Kirk, and A. R. Bell, "Quantum Radiation Reaction in Laser-Electron-Beam Collisions," Phys. Rev. Lett. 112, 015001 (2014).
- [65] Y. Kostyukov, I. Artemenko, and E. Nerush, "Growth rate of QED cascades in a rotating electric field," Probl. At. Sci. Technol. 116, 259 (2018).
- [66] S. Tang, B. King, and H. Hu, "Highly polarised gamma photons from electron-laser collisions," Phys. Lett. B 809, 135701 (2020).
- [67] G. Moortgat-Pick *et al.*, "Polarized positrons and electrons at the linear collider," Phys. Rep. **460**, 131–243 (2008).
- [68] Y.-F. Li, R. Shaisultanov, Y.-Y. Chen, F. Wan, K. Z. Hatsagortsyan, C. H. Keitel, and J.-X. Li, "Polarized Ultrashort Brilliant Multi-GeV γ Rays via Single-Shot Laser-Electron Interaction," Phys. Rev. Lett. **124**, 014801 (2020).
- [69] V. N. Baĭer, A. I. Mil'shteĭn, and V. M. Strakhovenko, "Interaction between a photon and an intense electromagnetic wave," Sov. Phys. J. Exp. Theor. Phys. **42**, 961–965 (1975).
- [70] V. Dinu, C. Harvey, A. Ilderton, M. Marklund, and G. Torgrimsson, "Quantum Radiation Reaction: From Interference to Incoherence." Phys. Rev. Lett. 116, 044801 (2016).
- [71] I. I. Artemenko, M. S. Krygin, D. A. Serebryakov, E. N. Nerush, and I. Yu Kostyukov, "Global constant field approximation for radiation reaction in collision of high-intensity laser pulse with electron beam," Plasma Phys. Control. Fusion **61**, 074003 (2019).